Brassica juncea plant cadmium resistance 1 protein (BjPCR1) facilitates the radial transport of calcium in the root

Won-Yong Song[a,b,c], Kwan-Sam Choi[c], De Angeli Alexis[a], Enrico Martinoia[a,b,1,2], and Youngsook Lee[b,1,2]

[a]Institute of Plant Biology, University of Zurich, CH-8008 Zurich, Switzerland; [b]Pohang University of Science and Technology-University of Zurich Cooperative Laboratory, Department of Integrative Bioscience and Biotechnology, World Class University Program, Pohang University of Science and Technology, Pohang 790-784, Korea; and [c]Division of Applied Biology, College of Agriculture and Life Sciences, Chungnam National University, Daejeon 305-764, Korea

Edited by Michael G. Palmgren, Centre for Membrane Pumps in Cells and Disease, Danish National Research Foundation, University of Copenhagen, Frederiksberg C, Denmark, and accepted by the Editorial Board October 14, 2011 (received for review March 28, 2011)

Calcium (Ca) is an important structural component of plant cell walls and an intracellular messenger in plants and animals. Therefore, plants tightly control the balance of Ca by regulating Ca uptake and its transfer from cell to cell and organ to organ. Here, we propose that *Brassica juncea* PCR1 (PCR1), a member of the plant cadmium resistance (PCR) protein family in Indian mustard, is a Ca^{2+} efflux transporter that is required for the efficient radial transfer of Ca^{2+} in the root and is implicated in the translocation of Ca to the shoot. Knock-down lines of *BjPCR1* were greatly stunted and translocated less Ca to the shoot than did the corresponding WT. The localization of BjPCR1 to the plasma membrane and the preferential expression of *BjPCR1* in the root epidermal cells of WT plants suggest that *BjPCR1* antisense plants could not efficiently transfer Ca^{2+} from the root epidermis to the cells located inside the root. Protoplasts isolated from *BjPCR1* antisense lines had lower Ca^{2+} efflux activity than did those of the WT, and membrane vesicles isolated from *BjPCR1*-expressing yeast exhibited increased Ca^{2+} transport activity. Inhibitor studies, together with theoretical considerations, indicate that BjPCR1 exports one Ca^{2+} in exchange for three protons. Root hair-specific expression of *BjPCR1* in *Arabidopsis* results in plants that exhibit increased Ca^{2+} resistance and translocation. In conclusion, our data support the hypothesis that BjPCR1 is an exporter required for the translocation of Ca^{2+} from the root epidermis to the inner cells, and ultimately to the shoot.

calcium translocation | plasma membrane H^+/Ca^{2+} antiporter | nutrition | calcium homeostasis

Calcium (Ca) is an essential nutrient for plants. It is required for Ca^{2+}-mediated signal transduction, the stabilization of the cell wall and plasma membrane, ion balance, and vacuolar osmoregulation (1–3). The diverse functions of Ca^{2+} in the plant require that the concentration of Ca^{2+} be maintained and regulated differently in different compartments, and in a timely manner, and this is achieved by the activity of numerous Ca transporters.

Ca^{2+}-mediated signal transduction is necessary for the proper response of plants to touch, cold, and drought, as well as for the closure of stomata in response to abscisic acid (ABA), cold, and atmospheric CO_2 (4, 5). Ca^{2+}-mediated signal transduction is often initiated by rapid Ca^{2+} influx through selective or nonselective Ca^{2+} channels located in the plasma membrane and intracellular organelles, such as the Ca^{2+}-permeable outward-rectifying K^+ channel, depolarization-activated Ca^{2+} channel, hyperpolarization-activated Ca^{2+} channel, and voltage-dependent Ca^{2+} channel (4, 5). In order that changes in Ca^{2+} concentration are perceived as a signal, the cytosolic Ca^{2+} concentration has to be maintained at submicromolar concentrations. Such a low cytosolic Ca^{2+} concentration can be maintained by Ca^{2+} efflux transporters, such as Ca^{2+}-ATPases (ECA1, ACA1, and ACA4) and H^+/Ca^{2+} antiporters (CAXs) at the endoplasmic reticulum membrane and tonoplast, respectively (2, 5), and Ca^{2+}-ATPases and H^+/Ca^{2+} exchangers at the plasma membrane (6, 7).

In contrast to this need of individual cells to maintain cytosolic Ca^{2+} at a very low level, large quantities of Ca^{2+} are needed at the whole-plant level because of the structural role that Ca^{2+} plays in stabilizing cell walls and the plasma membrane, as well as its function as a counter ion for the massive amount of anions in the vacuole. In crops, the drop of Ca^{2+} levels to below a critical level in fast-growing tissues causes diseases, such as black heart in *Apium graveolens* (celery), blossom end rot in *Solanum lycopersicum* (tomatoes), and bitter-pit in *Malus domestica* (apples) (1, 2). These phenomena demonstrate the importance of regulating Ca^{2+} uptake and allocation. In the root, Ca^{2+} is taken up by epidermal cells, radially transferred to the inner parts of the root, and then finally loaded into the xylem for transport to the shoot. However, a detailed understanding of the mechanism underlying each step of Ca^{2+} transport is lacking. For example, it has been debated which part of the root is involved in Ca^{2+} uptake from the rhizosphere and whether the apoplastic or symplastic pathway is the predominant route for Ca^{2+} transport across the endodermal layer of the root (8–10). It is also not known which transporters are necessary for xylem loading of Ca^{2+}.

In an effort to gain insight into the function of the plant cadmium resistance (PCR) family, we identified two members of this family from *Brassica juncea*. We demonstrate that, although *B. juncea* PCR1 (BjPCR1) exhibits strong sequence similarity to *Arabidopsis thaliana* PCR2 (AtPCR2), which plays a role in heavy metal transport (11, 12), BjPCR1 is not involved in heavy metal transport but contributes to Ca translocation from the root to the shoot via a Ca^{2+} efflux mechanism located in root epidermis.

Results

Identification of *B. juncea* PCRs. Previously, we identified and characterized two PCRs involved in heavy metal homeostasis in *Arabidopsis* (11, 12). *B. juncea* is a crop with a high intrinsic heavy metal tolerance and accumulation (13, 14), and it may therefore contain members of the PCR family with distinct characteristics. Because *Brassica* has coding sequences that are very similar to those of *A. thaliana* (15), we used primers specific for *AtPCR1* to isolate *PCR* genes from *B. juncea* (11). Using a genomic PCR approach, we identified three different *BjPCR*s. All three *BjPCR* genes have four exons and three introns at the same positions as *AtPCR1* and *AtPCR2* (Fig. S1). The lengths of the exons of the three *BjPCR* genes were very similar to those of

Author contributions: W.-Y.S., K.-S.C., E.M., and Y.L. designed research; W.-Y.S. performed research; W.-Y.S., K.-S.C., D.A.A., E.M., and Y.L. analyzed data; and W.-Y.S., D.A.A., E.M., and Y.L. wrote the paper.

The authors declare no conflict of interest.

This article is a PNAS Direct Submission. M.G.P. is a guest editor invited by the Editorial Board.

[1]E.M. and Y.L. contributed equally to this work.

[2]To whom correspondence may be addressed. E-mail: enrico.martinoia@botinst.uzh.ch or ylee@postech.ac.kr.

This article contains supporting information online at www.pnas.org/lookup/suppl/doi:10.1073/pnas.1104905108/-/DCSupplemental.

AtPCR1 and *AtPCR2*. In contrast, the introns exhibited some variation. *Brassica* PCR1 was more similar to AtPCR2 than to AtPCR1 and exhibited 76% identity at the amino acid level with AtPCR2 (Fig. 1*A*). Because of the high overall identity between AtPCR1, AtPCR2, and BjPCRs, particularly in the hydrophobic domain, which contains the CCXXXXCPC (CC-CPC) motif shown to be required for cadmium (Cd) resistance (11), we expected that BjPCRs would also be implicated in conferring Cd resistance. To test this hypothesis, we isolated the corresponding *BjPCR1* and *BjPCR2* cDNAs and expressed them in the Cd-sensitive yeast mutant DTY167. On normal half-strength synthetic galactose (SG)-agar medium, *BjPCR1*-, *BjPCR2*-, and *AtPCR2*-expressing yeast cells showed similar growth. Surprisingly, and in contrast to *Arabidopsis PCR2*, *BjPCR1* conferred only weak Cd tolerance and *BjPCR2* did not restore any tolerance at all to Cd (Fig. S2*A*). To determine why BjPCR1 does not confer Cd tolerance, we undertook domain-swapping experiments with BjPCR1 and AtPCR2. The results showed that mBP1, a hybrid construct consisting of the N-terminal part of AtPCR2 and the C-terminal part of BjPCR1, conferred Cd tolerance (Fig. S2*B*). Site-directed mutagenesis analysis within the N-terminal part of BjPCR1 revealed that the exchange of the naturally occurring Q11 with a His residue resulted in a BjPCR1 form that conferred Cd tolerance (Fig. S2*C*) and decreased Cd content (Fig. S2*D*) in *ycf1* yeasts. Interestingly, the single amino acid change, Q11H, caused a shift in the protein band mobility, although it did not change the BjPCR1 protein level (Fig. S2*E*). This band mobility shift suggests a change in protein structure that might have contributed to the dramatic change in PCR function to confer Cd tolerance.

Phenotypic Analysis of *BjPCR1* Antisense Lines. To investigate the physiological function of BjPCRs in *B. juncea*, we produced a silencing construct for *BjPCR1* and *BjPCR2* that down-regulated the expression of both genes. We examined *BjPCR1* and *BjPCR2* transcript levels in the roots of 20 transformants exhibiting bar gene-mediated phosphinothricin resistance, using RNA blot analysis with a *BjPCR1* probe that can cross-react with both *BjPCR* genes. Based on the expression levels of *BjPCRs* (Fig. 1*B*), we selected two lines with the lowest transcript levels (lines 5 and 17) and one where the transcript levels were only partially decreased and which could be used as a control (line 8). When these plants were grown under hydroponic conditions, lines 5 and 17 exhibited impaired growth, whereas line 8 grew at similar rates as the WT plants (Fig. 1*C*). Quantification of the shoot and root biomass confirmed our visual impression (Fig. 1*D*). In lines 5 and 17, the shoot biomass was decreased by nearly 40%. The reduction in biomass was even more pronounced at the root level, where the biomass of lines 5 and 17 decreased by more than 70% of WT values (Fig. 1*D*).

To determine the reason for this drastic phenotype, we first measured the levels of major cations in the mutant lines and WT plants grown under control conditions (Fig. 2 and Fig. S3). We did not detect any difference in cation content between our control anti–BjPCR1-8 plant and the WT, which corresponded well with the absence of a difference in growth phenotype in this line. In contrast, we observed a pronounced difference in Ca, iron (Fe), manganese (Mn), and sodium (Na) concentrations between anti–BjPCR1-5 and anti–BjPCR1-17 and the corresponding WT (Fig, 2*A* and Fig. S3 *A*–*D*). Only a slight effect was detected for Mg^{2+}, whereas no differences were observed for zinc (Zn), copper (Cu), and potassium (K) (Fig. 2*B* and

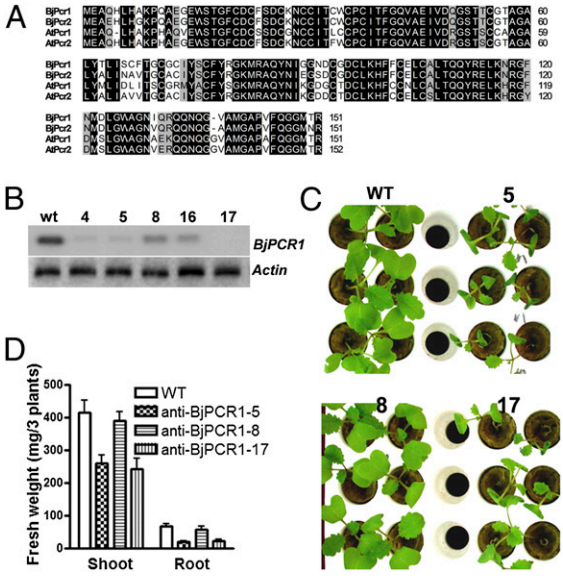

Fig. 1. Characterization of BjPCR1. (*A*) Comparison of PCRs of *A. thaliana* and *B. juncea* by amino acid sequence alignment. Identical or similar amino acid residues are shown in black or gray boxes. ClustalW (http://align.genome.jp) was used to generate the alignment. (*B–D*) Phenotype analysis of *BjPCR1* knock-down mutants. (*B*) Transcription levels of *BjPCR1* in WT (wt) and anti-BjPCR1 *B. juncea* (lines 4, 5, 8, 16, and 17) plants. (*C*) Growth of 2-wk-old WT and anti-BjPCR1 (lines 5, 8, and 17) plants in hydroponic culture. (*D*) Fresh weight of the shoots and roots of WT and anti-BjPCR1 (lines 5, 8, and 17) plants grown as shown in *C*. The average ± SE is shown (n = 20, N = 3).

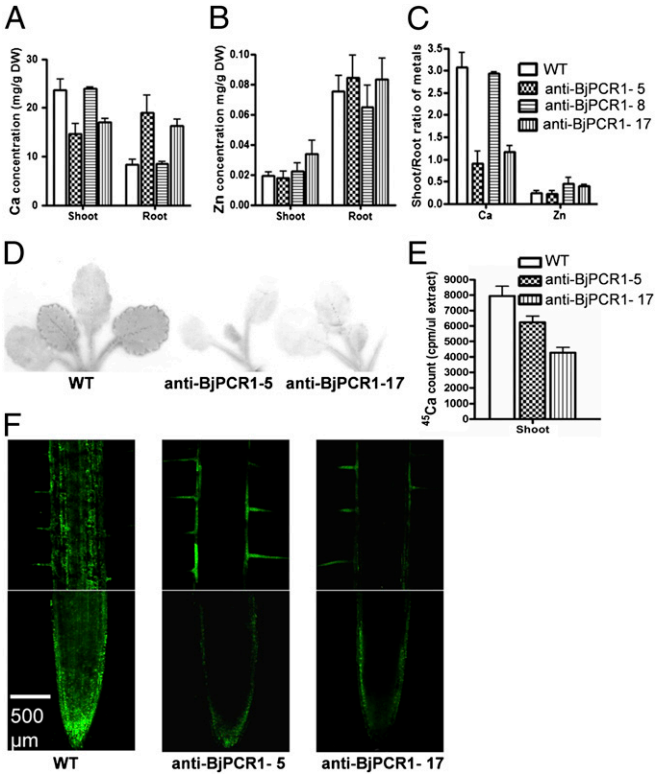

Fig. 2. *BjPCR1* antisense lines exhibited reduced translocation of Ca^{2+} to the shoot and reduced radial translocation of Ca^{2+} to the inner part of the root. Ca (*A*) and Zn (*B*) concentrations in the shoots and roots of 4-wk-old WT and anti-BjPCR1 *B. juncea* plants. DW, dry weight. (*C*) Shoot-to-root ratios of Ca and Zn concentrations as shown in *A* and *B*. (*D*) Autoradiography of 3-wk-old *B. juncea* plants incubated in hydroponic medium supplemented with 1.5 mM $CaCl_2$ containing 0.4 MBq of $^{45}CaCl_2$ supplied through the root for 15 h. (*E*) Counts of ^{45}Ca normalized by the volume of cell sap extracted from the shoot of plants treated with $^{45}CaCl_2$ as in *D*. All data represent average ± SE (n = 5, N = 2). (*F*) Distribution of free Ca^{2+} in the roots of the WT and anti-BjPCR1 lines visualized using fluo-3 fluorescence. Roots of 5-d-old *B. juncea* plants were stained with fluo-3 for 4 h, washed with PBS solution, and observed by confocal microscopy. (Scale bar = 500 μm.)

Fig. S3 *E* and *F*). The most drastic differences between the silenced lines and WT plants were observed for Ca (Fig. 2*A*). Ca concentrations in anti–BjPCR1-5 and anti–BjPCR1-17 were only 65–75% of those observed in the WT, whereas they were at least twofold higher than in the WT in the root. Consequently, the shoot-to-root ratio of Ca^{2+} was dramatically altered in the anti–BjPCR1-5 and anti–BjPCR1-17 lines, whereas that of other ions was less affected (Fig. 2*C* and Fig. S3*G*). A comparison of biomass (Fig. 1*D*) with Ca concentrations (Fig. 2*A*) revealed that the growth of roots of the antisense lines was strongly impaired despite the fact that they contained high levels of Ca^{2+}. This may be because the high level of Ca^{2+} exerted a toxic effect or the shoot, which did not have sufficient levels of Ca^{2+}, could not develop normally, and thus failed to provide sufficient energy for root growth. The remarkable difference in the shoot-to-root ratio of Ca between the WT and the antisense lines 5 and 17 indicated that BjPCR1 plays a major role in the transfer of Ca^{2+} from the root to the shoot, and thus differs from its *Arabidopsis* homolog, AtPCR2, which transports Zn (12). Therefore, we concentrated our further studies on the role of BjPCR1 in Ca^{2+} distribution and transport.

Ca^{2+} Translocation in Anti-BjPCR1 Lines. To confirm the decreased root-to-shoot Ca translocation observed in the BjPCR1-5 and BjPCR1-17 lines, we performed short-term uptake experiments using $^{45}Ca^{2+}$ (Fig. 2 *D* and *E*). When grown in hydroponic medium and exposed for 15 h to 0.4 MBq of $^{45}Ca^{2+}$, the leaves of the anti-BjPCR1 mutant lines 5 and 17 contained less ^{45}Ca radioactivity than did those of the corresponding WT (Fig. 2 *D* and *E*). To test if BjPCR1 is involved in the lateral transport of Ca^{2+}, we analyzed Ca^{2+} distribution in the root hair zone and root tip, where the Casparian band has not yet formed, using a cell-permeable Ca^{2+} dye, the acetoxymethyl ester derivative of fluo-3 (Fluo-3-AM; Molecular Probes). This dye permeates into cells and is hydrolyzed by nonspecific esterases, and the cleavage product, fluo-3, emits a green fluorescence when bound to Ca^{2+}, allowing the visualization of intracellular Ca^{2+} (13). Roots of WT plants exhibited a strong Ca^{2+}-dependent fluorescence signal in the tip and epidermal layer of the tip (Fig. 2*F*). A Ca^{2+} signal was also observed in the stele. In the root hair zone of the root, the strongest Ca^{2+} signal was observed in the tissue inside the epidermis adjacent to the root tip and in the stele (Fig. 2*F*). In contrast, the Ca^{2+}-dependent fluorescence signal of the two anti-BjPCR1 mutant lines was less pronounced in the root tip. In the root hair zone, Ca^{2+}-dependent fluorescence could only be observed in the epidermal cells and root hairs but not in the stele (Fig. 2*F* and Fig. S4). No difference in the fluorescence pattern of zinpyr-1 (Sigma–Aldrich), an indicator dye for Zn, was observed between the roots of the WT and the antisense lines (Fig. S5), which corresponded to the absence of differences in Zn concentration in WT and mutant plants (Fig. 2*B*). Furthermore, this result indicates that the difference in the fluo-3 pattern between the antisense and WT lines did not originate from any difference in dye penetration. Taken together, these results suggest that anti-BjPCR1 lines do not efficiently translocate Ca^{2+} from the root epidermal cells to the inner cells of the root.

Tissue-Specific Expression of *BjPCRs*. To understand the function of *BjPCR1* and *BjPCR2* in *Brassica* further, we analyzed the tissue-specific expression. *BjPCR1* was expressed mainly in roots but was also present in leaves (Fig. 3*A*). Expression in stems and flowers was low. The expression pattern of *BjPCR2* was similar to that of *BjPCR1*, but the overall expression level was lower than that of *BjPCR1* (Fig. 3*A*). To obtain a clue as to where in the root *BjPCR1* and *BjPCR2* are expressed, we first used a stepwise grinding method. *BjPCR1* was highly expressed in root hair cells, which fell off at the first step of grinding, and its expression pattern was similar to that of *EXP7*, a root hair marker (14), but was opposite to that of *HMA4*, which is mainly expressed in vascular tissues (15) (Fig. 3*B*). Whole-mount in situ RNA

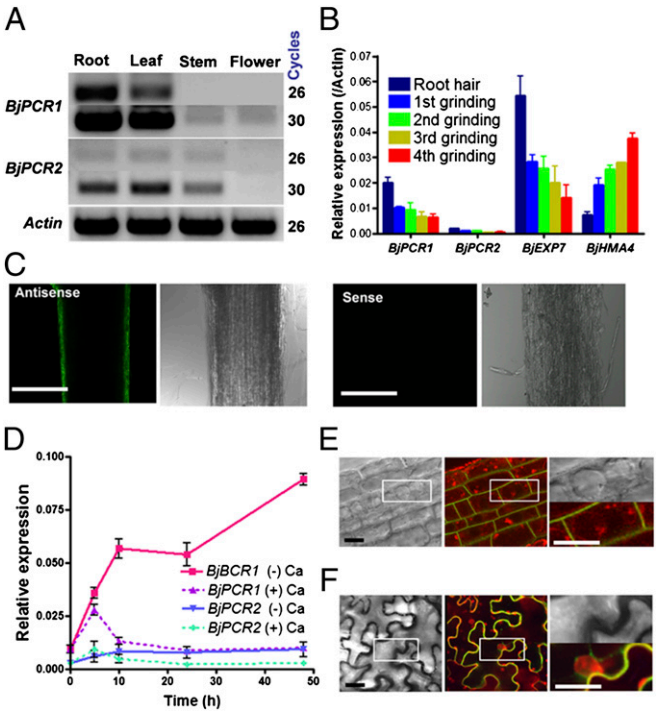

Fig. 3. Expression pattern and subcellular localization of BjPCR1. (*A*) RT-polymerase chain reaction analysis of *BjPCR1* and *BjPCR2* in *B. juncea* plants. (*B*) Localization of *BjPCR1* and *BjPCR2* transcripts in the roots of B. *juncea* grown on agar medium for 5 d. *BjEXP7* and *BjHMA4* were used as marker genes that are expressed in root hairs and vascular tissue, respectively. Root cell layers were collected in liquid nitrogen, sequentially ground four times, and collected again, and their mRNA was extracted as described in *SI Materials and Methods*. The average ± SE is shown ($n = 3$, $N = 2$). (*C*) Localization of *BjPCR1* in the roots of *B. juncea*, as detected by the whole-mount in situ RNA hybridization technique, using a fluorescein-12-UTP–labeled antisense (*Left*) or sense (*Right*; background control) probe. Optically sectioned images of the median planes of the samples were obtained by confocal microscopy. (Scale bars = 500 μm.) (*D*) Expression pattern of *BjPCR1* and *BjPCR2* under excess (10 mM $CaCl_2$) and deficient (0 mM $CaCl_2$) Ca conditions. The average ± SE is shown ($n = 3$, $N = 2$). (*E* and *F*) Plasma membrane localization of BjPCR1-GFP. (*E*) Fluorescence at the root epidermis of a BjPCR1-GFP transgenic *Arabidopsis* plant. The red fluorescence indicates the vacuoles and endosomes stained with FM4-64. (Scale bar = 5 μm.) (*F*) Fluorescence of BjPCR1-GFP at the leaf epidermis of a BjPCR1-GFP–expressing tobacco plant. Red fluorescence indicates the cell walls and nuclei of epidermal cells stained with propidium iodide. Bright-field images (*Left*), merged images of red fluorescence and green fluorescence (*Center*), and images enlarged from the boxed areas in the first two columns (*Right*). (Scale bar = 5 μm.)

hybridization confirmed that *BjPCR1* is indeed strongly expressed in the epidermal layer (antisense probe of Fig. 3*C*). We cannot completely exclude the possibility that *BjPCR1* is also expressed in other parts of the root; however, in this case, the expression level would be very low compared with that in epidermal cells. The grinding method indicates that *BjPCR2* exhibits a similar expression pattern as *BjPCR1* (Fig. 3*B*), but the expression level of *BjPCR2* was 1/10th that of *BjPCR1* (Fig. 3 *A*, *B*, and *D*). *BjPCR1* was strongly induced under Ca^{2+} starvation conditions but not under Ca^{2+} excess conditions (Fig. 3*D*). *BjPCR2* exhibited a similar response, but its expression level remained lower than that of *BjPCR1*.

Plasma Membrane Localization of BjPCR1-GFP. To investigate the subcellular localization of BjPCR1 *in planta*, transgenic *Arabidopsis* lines expressing the *35S::BjPCR1-GFP* construct were generated. Green fluorescence in the root epidermal cells of these plants was localized to the plasma membrane (Fig. 3*E*).

Transient expression of the construct in tobacco epidermal cells by infiltration confirmed that BjPCR1-GFP was targeted to the cell surface in close proximity to the cell wall, which was stained with propidium iodide (Fig. 3*F*). These results indicate that BjPCR1-GFP is located at the plasma membrane of plant cells.

Ca^{2+} Transfer by BjPCR1 in the Root Epidermis. Ca^{2+} transport analysis and epidermal plasma membrane localization of BjPCR1 indicated that BjPCR1 acts as a Ca^{2+} efflux transporter at the epidermis for shoot Ca^{2+} translocation in *B. juncea*. If BjPCR1 indeed facilitates Ca^{2+} efflux from the epidermis to the apoplast, the pathway for Ca^{2+} translocation to the shoot involves both the symplast of the epidermal cells and the adjacent apoplast. To estimate the portions of the apoplast/symplast combinatorial pathway and the entirely apoplastic pathway in the total transfer of Ca^{2+} to the shoot, we compared the short-term root uptake of ^{45}Ca at 0 °C and 25 °C. The results demonstrated that, although Ca^{2+} transport was significant at 0 °C (70% for WT), which is probably through the apoplast alone, 30% of the transport is mediated by energy-dependent mechanism(s) that might include uptake into the epidermis and subsequent release into the cortical apoplast (Fig. S6, WT). Furthermore, the same temperature-dependent transport assays with antisense BjPCR1 lines 5 and 17 revealed that they contained higher levels of Ca^{2+} than the WT, especially at 25 °C (Fig. S6), which suggests that BjPCR1 is important for the energy-dependent removal of Ca^{2+} from the epidermis to the apoplast.

To test further whether Ca^{2+} is indeed a physiological substrate of BjPCR1 important for Ca^{2+} transfer at the epidermis, we expressed *BjPCR1* in *Arabidopsis* root hair cells using the *AtEXP7* promoter, and thereby generated *EXP2p::BjPCR1-V5* and *EXP2p::BjPCR1-GFP* transgenic plants. As shown in Fig. 4*A*, BjPCR1-GFP was indeed specifically expressed in the root hair cells of these *Arabidopsis* plants. When *EXP2p::BjPCR1-V5* or *EXP2p::BjPCR1-GFP* transgenic *Arabidopsis* plants were grown on media containing different concentrations of Ca, Mn, or Fe, *Arabidopsis* plants expressing *BjPCR1* grew better than WT under the Ca^{2+}-deficient, Ca^{2+}-sufficient, Ca^{2+}-excessive, and Mn^{2+}-excessive conditions but grew similar to WT in medium containing excess Fe (Fig. 4*B* and Fig. S7 *A*, *B*, and *E*). The most dramatic effect was observed when Ca^{2+} was present at high concentrations, which impaired plant growth (Fig. 4*B* and Fig. S7 *A* and *B*). Ca^{2+} was present at higher concentrations in the shoots but at similar concentrations in the roots of transgenic *Arabidopsis* lines relative to the WT (Fig. S7*C*), resulting in an increase in shoot-to-root Ca ratio in the transgenic plants (Fig. 4*C*) and indicating that Ca^{2+} is translocated more efficiently in the transgenic plants. Together, these results indicate that Ca^{2+} is a physiological substrate of BjPCR1, and they further suggest that, in the epidermis, BjPCR1 contributes to Ca^{2+} translocation to the shoot.

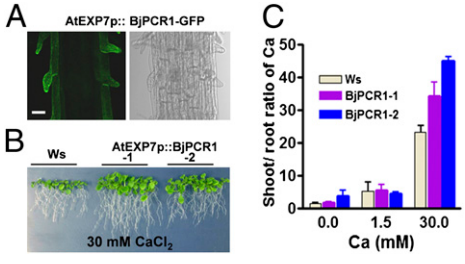

Fig. 4. *Arabidopsis* lines expressing *BjPCR1* in root hairs exhibited enhanced Ca resistance and translocation to the shoot. (*A*) Root hair-specific localization of *BjPCR1* in *EXP7promoter::BjPCR1-GFP* transgenic *Arabidopsis*. (Scale bar = 5 μm.) (*B*) Ca tolerance phenotype of *EXP7promoter::BjPCR1* transgenic *Arabidopsis* lines (EXP7p::BjPCR1-1 and BjPCR1-2). Plants were grown on 30 mM $CaCl_2$ containing half-strength Murashige and Skoog medium for 3 wk. Ws, WT plants. (*C*) Shoot-to-root Ca ratio in *EXP7promoter::BjPCR1*-expressing *Arabidopsis* lines (BjPCR1-1 and BjPCR1-2). Ca content was measured, and the shoot-to-root Ca ratio was analyzed using data from Fig. S7*C*. Average values ± SE are shown (n = 3, N = 2).

Ca^{2+} Efflux Activity by BjPCR1. To test whether BjPCR1 acts directly as a Ca^{2+} efflux transporter, we performed transport experiments using mesophyll protoplasts isolated from the anti-BjPCR1 lines and WT plants. The $^{45}Ca^{2+}$ uptake activity of protoplasts of the antisense lines was about twice that of control protoplasts (Fig. 5*A*). This result could indicate that the Ca^{2+} taken up by control plants is readily exported, whereas that taken up by antisense lines is not. To test this hypothesis, we preloaded protoplasts isolated from control and mutant plants for 30 min with $^{45}Ca^{2+}$ and then investigated the release of $^{45}Ca^{2+}$. Indeed, Ca^{2+} efflux rates were slower in protoplasts isolated from antisense lines than in those from WT plants (Fig. 5*B*), indicating that BjPCR1 acts as a Ca^{2+} efflux transporter and supporting the conclusions drawn from the experiments on whole plants.

To confirm further that BjPCR1 is indeed a Ca^{2+} transporter, we expressed *BjPCR1* in the yeast strain SM17, which is deficient in CNB1 and the Ca^{2+} transporters PMR1, PMC1, and VCX1. The ^{45}Ca uptake experiment in the *BjPCR1*-expressing yeast cells showed that BjPCR1 decreased the Ca^{2+} content of the cell (Fig. S8*A*), which indicated that BjPCR1 had a role in Ca^{2+} efflux. This result is also consistent with the increased Ca^{2+} level in protoplasts isolated from anti-BjPCR1 lines (Fig. 5*A*). For the in-depth analysis of BjPCR1-mediated transport, vesicles were isolated from yeast cells and used in the Ca^{2+} transport assay. The vesicles prepared from yeast cells expressing BjPCR1 exhibited significantly increased Ca^{2+} transport activity relative to those isolated from the empty vector control. During the first 30 min of incubation, yeast vesicles expressing BjPCR1 took up Ca^{2+} about fourfold faster than the empty vector control (Fig. 5*C*). This activity demonstrates Ca^{2+} efflux in vivo, because only the inside-out vesicles can use the magnesium (Mg)-ATP required to drive the transport. To exclude the possibility that the difference observed was attributable either to variation in the stability of vesicles or to the amount of vesicles used, we performed a control experiment using leukotriene, which is glutathionated and taken up by ABCC-type transporters in yeast. We did not see any difference in leukotriene uptake activity between the two preparations (Fig. S8*B*). Concentration-dependent Ca^{2+} transport assays revealed that BjPCR1 is a high-capacity and low-affinity Ca^{2+} transporter exhibiting an apparent K_m of 50 μM (Fig. S8*C*). To determine substrate specificity, competition of $^{45}Ca^{2+}$ transport assay was performed using cold Ca^{2+}, Fe^{2+}, and Mn^{2+}. The $^{45}Ca^{2+}$ transport activity was inhibited by 93% and 38% by addition of 500 μM Ca^{2+} and Mn^{2+} but not by 500 μM Fe^{2+} (Fig. S8*D*). The result suggests that Ca^{2+} is a preferred substrate for BjPCR1 compared with other ions.

To determine how the BjPCR1-mediated Ca^{2+} transport was energized, we performed inhibitor studies (Fig. 5*D*). Vanadate, an inhibitor of P-type ATPases, such as the plasma membrane proton pump, inhibited the transport by 80% compared with the Mg-ATP control, suggesting that the plasma membrane-localized H^+-ATPase generates the driving force for Ca^{2+} uptake. To test this hypothesis, we first examined the effect of ammonium chloride, which abolishes the ΔpH but not the membrane potential ($\Delta\psi_m$). In the presence of 5 mM ammonium chloride, Ca^{2+} transport was inhibited by 34%. This result indicated that BjPCR1-mediated Ca^{2+} uptake into yeast vesicles is partially ΔpH-dependent and that BjPCR1 does not act as a simple Ca^{2+} channel. To identify the additional driving force that supports the BjPCR1-mediated Ca^{2+} fluxes, we performed Ca^{2+} uptake experiments in the presence of valinomycin, which dissipates the $\Delta\psi_m$. In this case, Ca^{2+} transport was inhibited by 51%, indicating that Ca^{2+} transport is electrogenic. Finally, the addition of carbonyl cyanide m-chlorophenylhydrate, which disrupts both the ΔpH and $\Delta\psi_m$, had a drastic effect and inhibited Ca^{2+} transport activity by 99%. Two additional experiments provided further confirmation that the proton motive force drives BjPCR1-

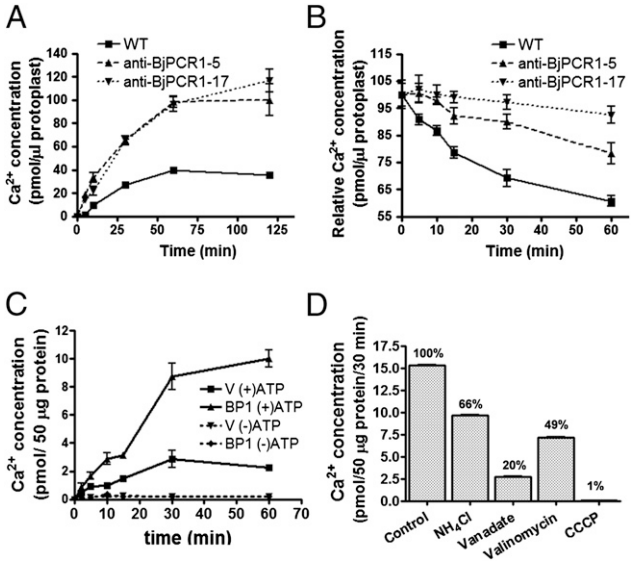

Fig. 5. Ca^{2+} transport mediated by BjPCR1. (*A*) Time-dependent Ca^{2+} uptake by protoplasts of WT and anti–BjPCR1-5 and anti–BjPCR1-17. The protoplasts were suspended in loading buffer containing 100 μM $CaCl_2$, 18.5 kBq of $^{45}CaCl_2$, and 18.5 kBq of ^3H_2O, and they were then incubated for the indicated periods of time. Only the intact protoplasts were collected by centrifugation. (*B*) Time-dependent release of Ca^{2+} from protoplasts of WT and anti-BjPCR1 plants. The protoplasts were preloaded in medium containing 100 μM $CaCl_2$ and 18.5 kBq of $^{45}CaCl_2$ for 30 min, washed briefly with ice-cold bathing solution, and incubated in the bathing medium. Only intact cells were collected, and radioactive disintegrations from the samples were counted. The Ca^{2+} content was normalized against the ^3H_2O content of the protoplasts. The average ± SE is shown (n = 4, N = 3). (*C* and *D*) Ca^{2+} uptake experiment in yeast microsomes isolated from *Saccharomyces cerevisiae* transformed with the empty vector (V) or BjPCR1 (BP1). (*C*) Time course of Ca^{2+} uptake by vesicles from cells transformed with V or BP1. Ca^{2+} uptake was performed in the absence (–ATP) or presence (+ATP) of 4 mM Mg-ATP in Ca transport medium containing a standard transport buffer at 25 °C for the indicated period. The microsomes were collected by filtration on a nitrocellulose filter. (*D*) Effects of inhibitors of ion transport on Ca^{2+} uptake by vesicles derived from BP1-expressing cells. Uptake assay was performed using yeast microsomes expressing V or BP1 in the Ca^{2+} transport medium containing 4 mM Mg-ATP (Control) plus the compounds indicated [i.e., NH_4Cl, 5 mM; vanadate, 1 mM; valinomycin, 2 μM; carbonyl cyanide m-chlorophenylhydrate (CCCP), 10 μM]. The bars represent the Ca^{2+} concentrations in vesicles expressing BjPCR1 minus those in vesicles transformed with empty vector (n = 4, N = 2). The values (%) in the graph are the rates of uptake expressed as a percentage of the control. Average values ± SE are shown (n = 3, N = 2).

mediated Ca^{2+} transport: (*i*) Preincubation with Mg-ATP resulted in faster Ca^{2+} uptake into yeast vesicles (Fig. S8*E*), and (*ii*) yeast vesicles expressing BjPCR1 exhibited a more pronounced recovery of pH when challenged with Ca^{2+}, as indicated by the larger increase in 9-amino-6-chloro-2-methoxyacridine (ACMA) fluorescence in BjPCR1-expressing yeast microsomes than in empty vector (EV)-expressing ones (Fig. S8*F*). In this experiment, low pH-induced quenching of ACMA fluorescence was transiently reversed by the addition of Ca^{2+} to the medium, which is most likely attributable to H^+ release by Ca^{2+}/H^+ antiport activity. Together, these results indicate that Ca^{2+} transport by BjPCR1 is driven by a proton-coupled antiport mechanism. Because proton transport into vesicles by H^+-ATPase generates an inside-positive membrane potential and a collapse of the membrane potential by valinomycin-inhibited Ca^{2+} uptake into the vesicles, it is likely that more positive charges are exported than imported by BjPCR1 in the vesicle membrane (i.e., more charges carried by H^+ efflux than by Ca^{2+} influx; see below). This hypothesis is confirmed by a theoretical consideration, which, based on the following equation (details are provided in *SI Materials and Methods*),

$$E_{eq}^{exch} = \frac{1}{r-2}\left(rE_{H^+} - 2E_{Ca^{2+}}\right) \quad [1]$$

where r is the stoichiometric coefficient of the exchange mechanism (rH^+:Ca^{2+}), and E_{H+} and $E_{Ca}{}^{2+}$ are the Nernst potential of H^+ and Ca^{2+}, respectively, shows that in the physiological ranges (Fig. S9*B*, shadowed area), the exchanger can always mediate Ca^{2+} efflux when one Ca^{2+} is exchanged with three protons.

Discussion

In this study, we demonstrated that BjPCR1, a homolog of AtPCR2, exports Ca^{2+} from plant cells and acts as a Ca^{2+} transporter in plant protoplasts and membrane vesicles isolated from yeast cells. AtPCR1 and AtPCR2 are small proteins that contain two predicted membrane-spanning α-helices and contribute to Cd resistance and Zn homeostasis, respectively (11, 12). The PCR family of genes, characterized by the common cysteine-rich PLAC8 domain, belongs to a large gene family that consists of many members in eukaryotes, including fungi, green algae, plants, and animals (16, 17). Two completely different functions have been associated with this gene family. On the one hand, the encoded proteins have been shown to act as transporters of Zn and Cd (11, 12), and on the other, they have been associated with the control of the number of cells in fruits (16, 18).

Although BjPCRs are highly similar in amino acid sequence to their *Arabidopsis* counterparts AtPCR1 and AtPCR2, antisense lines for *BjPCR1* were not compromised in Zn translocation; however, surprisingly, they exhibited reduced translocation of Ca^{2+} to the shoot, which resulted in impaired growth. The impaired Ca^{2+} translocation into the shoot from the root of *BjPCR1* antisense lines 5 and 17 is likely attributable to the impaired transfer of Ca^{2+} from the epidermal cells, where *BjPCR1* is highly expressed, to the inner cells of the root, as evidenced by the accumulation of fluo-3 signal at the root epidermis of the antisense lines (Fig. 2*F*). Interestingly, in *Arabidopsis*, the Ca concentration in roots seemed to be tightly controlled through Ca^{2+} translocation to the shoot, because *Arabidopsis* lines grown on low and high Ca^{2+} concentrations exhibited similar Ca^{2+} concentration in the roots, whereas the shoots of plants grown on higher Ca^{2+} concentrations contained higher Ca^{2+} concentrations than those grown on lower Ca^{2+} concentrations (Fig. S7*D*). Thus, under high Ca^{2+} concentration conditions, *Arabidopsis* plants expressing *BjPCR1* in the epidermis translocated more Ca from the root to the shoot, which contributed to their improved Ca tolerance (Fig. 4), most likely attributable to dilution effect. Together, these results indicate that the extrusion of Ca^{2+} by BjPCR1 from the epidermal cells to the apoplast of the cortical layer of the root is required for the efficient movement of Ca^{2+} from the root to the shoot. In addition, our temperature-dependent Ca^{2+} transport assay (Fig. S6) revealed that the antisense BjPCR1 plants retained more Ca^{2+} in the root than the WT, indicating that the energy-dependent activity of BjPCR1 is responsible for the removal of Ca^{2+} from the root. Because there is no extensive symplastic connection via plasmodesmata between the epidermal and cortical layers of cells in the root (19, 20), BjPCR1 is expected to remove Ca^{2+} to the apoplast of the root, and thereby contributes to the translocation of Ca^{2+} from the root to the shoot. There is some debate on whether Ca^{2+} is delivered to the xylem by the apoplastic or symplastic pathway across the endodermal layer of the root (1, 8, 21, 22). So far, the available data indicate that Ca^{2+} uptake and transfer to the xylem are achieved by a complex mechanism, which is highly regulated and may differ from one plant to another. However, at least in *B. juncea*, it is clear from our results that apoplastic transfer of Ca^{2+} at the interface of epidermal/cortical cells is an important step in the radial transfer of Ca^{2+} across the root. A similar function in radial translocation

of metal ions at the root epidermis has been described for AtPCR2 (12). AtPCR2 is a Zn efflux transporter located at the plasma membrane of root xylem cells and epidermal cells, and an *AtPCR2* knockout mutant exhibited reduced Zn translocation to shoots. Thus, efflux transport systems may be required for the radial transfer of mineral ions from epidermal to inner layers through the apoplastic pathway.

No transporter has yet been shown to be responsible for the radial transport of Ca^{2+} in the root. Plant roots need to transport high levels of Ca^{2+} in a radial direction from the epidermis to the vascular tissue, because shoots require a large amount of Ca^{2+} (4). To translocate high levels of Ca^{2+} through the epidermal cells to the inner part of a root, a high-capacity Ca^{2+} transporter, such as a plasma membrane-localized CAX or Na^+/Ca^{2+} exchanger (NCX), has been postulated to exist, because epidermal cells do not contain enough plasmodesmata for an efficient symplasmic transfer of Ca^{2+}. In mammals, an Na^+/Ca^{2+} exchanger (NCX) prevents significant increases in intracellular Ca^{2+} by exhibiting low-affinity and high-capacity efflux activity (23). In plants, the presence of plasma membrane-localized CAXs was suggested based on a biochemical assay that used plasma membrane-derived vesicles from *Zea mays* (corn) leaves and roots; however, no plasma membrane-localized CAX gene has yet been reported in plants (6, 7). Ca^{2+} transport assays using BjPCR1-expressing yeast vesicles imply that BjPCR1 can function as a high-capacity and low-affinity H^+/Ca^{2+} exporter. Experiments with agents abolishing the ΔpH, $\Delta\Psi$, or both, together with theoretical considerations, revealed that using a stoichiometry of at least three protons per exported Ca^{2+}, BjPCR1 can efficiently export Ca^{2+} from the cell. A mammalian NCX (24, 25) has a stoichiometry of $3Na^+/Ca^{2+}$ or $4Na^+/Ca^{2+}$, whereas for a vacuolar Ca^{2+} proton antiporter, a stoichiometry of $3H^+/Ca^{2+}$ has been postulated (26). Furthermore, studies of a CAX from *Escherichia coli* also pointed to a stoichiometry higher than $2H^+/Ca^{2+}$ (27).

Although Ca^{2+} is available in sufficient amounts in the soil, Ca-related disorders, such as bitter pit in apple fruit, blossom-end rot in tomato fruit, and tip burn in the leaves of vegetables, can occur, especially in vigorously growing plants and in parts of the plant that demand a high level of Ca^{2+}. It is therefore likely that these plants are limited in their ability to transfer Ca^{2+} to the above-ground parts and that genetically engineering crops with BjPCR1 might improve the quality and yield of these plants.

In addition to acting as cation transporters, members of the PLAC8 motif-containing family have been associated with the control of cell number (16, 18). Therefore, it remains an open question as to whether other genes that contain the common PLAC8 motif regulate cell number through the transport of divalent cations in a manner similar to other members of the PCR family. The fact that PCRs act as transporters of the classic signaling compound Ca^{2+} (in the case of BjPCR1) and the important enzyme cofactor Zn^{2+} (in the case of AtPCR2) may indicate that cell number is also adjusted by the transport of such cations.

Materials and Methods

The *B. juncea* 182921 line (28) was grown on rock-wool block containing hydroponic nutrient solution (*SI Materials and Methods*). For the $^{45}CaCl_2$ uptake experiment, anti-BjPCR1 lines and WT *B. juncea* plants were grown in half-strength hydroponic medium for 3 wk. The plants were then incubated in hydroponic nutrient solution supplemented with 0.4 MBq of $^{45}CaCl_2$ for 5 and 12 h, and shoots were separated from the roots. The radioactivity was measured using a liquid scintillation counter (Perkin–Elmer). Autoradiography of $^{45}CaCl_2$ was performed on plants incubated in medium supplemented with 0.4 MBq of $^{45}CaCl_2$ for 12 h. Other methods are described in *SI Materials and Methods*.

ACKNOWLEDGMENTS. We thank Dr. Armando Carpaneto for performing the oocyte experiments and Prof. Ueli Grossniklaus for help in initial in situ hybridization experiments. This work was supported by Grant K20607000006 from the Global Research Laboratory program of the Ministry of Education, Science, and Technology of Korea (to Y. L. and E. M.); Grant R31-10105 from the World Class University program through the National Research Foundation of Korea funded by the Ministry of Education, Science, and Technology; Grant PJ0074482011 from the Cooperative Research Program of Rural Development Administration (to Y.L.); Grant FOOD-CT-2006-0016253 from the European Union project PHIME (Public health aspects of long-term, low-level mixed element exposure in susceptible population strata) (to E.M.); and European Molecular Biology Organization Fellowship ALTF 872009 (to D.A.A.).

1. Marschner H (1995) *Mineral Nutrition of Higher Plants* (Academic, San Diego).
2. White PJ, Broadley MR (2003) Calcium in plants. *Ann Bot (Lond)* 92:487–511.
3. Maathuis FJM (2009) Physiological functions of mineral macronutrients. *Curr Opin Plant Biol* 12:250–258.
4. White PJ, Bowen HC, Demidchik V, Nichols C, Davies JM (2002) Genes for calcium-permeable channels in the plasma membrane of plant root cells. *Biochim Biophys Acta* 1564:299–309.
5. Kudla J, Batistič O, Hashimoto K (2010) Calcium signals: The lead currency of plant information processing. *Plant Cell* 22:541–563.
6. Kasai M, Muto S (1990) Ca^{2+} pump and Ca^{2+}/H^+ antiporter in plasma membrane vesicles isolated by aqueous two-phase partitioning from corn leaves. *J Membr Biol* 114(2):133–142.
7. Vicente JAF, Vale MGP (1995) Activities of Ca^{2+} pump and low affinity Ca^{2+}/H^+ antiport in plasma membrane vesicles of corn roots. *J Exp Bot* 46:1551–1559.
8. White PJ (2001) The pathways of calcium movement to the xylem. *J Exp Bot* 52: 891–899.
9. Cholewa E, Peterson CA (2004) Evidence for symplastic involvement in the radial movement of calcium in onion roots. *Plant Physiol* 134:1793–1802.
10. Hayter ML, Peterson CA (2004) Can Ca^{2+} fluxes to the root xylem be sustained by Ca^{2+}-ATPases in exodermal and endodermal plasma membranes? *Plant Physiol* 136: 4318–4325.
11. Song WY, et al. (2004) A novel family of cys-rich membrane proteins mediates cadmium resistance in Arabidopsis. *Plant Physiol* 135:1027–1039.
12. Song WY, et al. (2010) Arabidopsis PCR2 is a zinc exporter involved in both zinc extrusion and long-distance zinc transport. *Plant Cell* 22:2237–2252.
13. Zhang WH, Rengel Z, Kuo J (1998) Determination of intracellular Ca^{2+} in cells of intact wheat roots: Loading of acetoxymethyl ester of fluo-3 under low temperature. *Plant J* 15:147–151.
14. Cho HT, Cosgrove DJ (2002) Regulation of root hair initiation and expansin gene expression in Arabidopsis. *Plant Cell* 14:3237–3253.
15. Hussain D, et al. (2004) P-type ATPase heavy metal transporters with roles in essential zinc homeostasis in Arabidopsis. *Plant Cell* 16:1327–1339.
16. Guo M, et al. (2010) Cell Number Regulator1 affects plant and organ size in maize: Implications for crop yield enhancement and heterosis. *Plant Cell* 22:1057–1073.
17. Song WY, Hörtensteiner S, Tomioka R, Lee Y, Martinoia E (2011) Common functions or only phylogenetically related? The large family of PLAC8 motif-containing/PCR genes. *Mol Cells* 31(1):1–7.
18. Frary A, et al. (2000) fw2.2: A quantitative trait locus key to the evolution of tomato fruit size. *Science* 289(5476):85–88.
19. Zhu T, Lucas WJ, Rost TL (1998) Directional cell-to-cell communication in the Arabidopsis root apical meristem. I. An ultrastructural and functional analysis. *Protoplasma* 203(1-2):35–47.
20. Ma F, Peterson CA (2001) Frequencies of plasmodesmata in Allium cepa L. roots: Implications for solute transport pathways. *J Exp Bot* 52:1051–1061.
21. McLaughlin SB, Wimmer R (1999) Calcium physiology and terrestrial ecosystem processes. *New Phytol* 142:373–417.
22. Yang HQ, Jie YL, Zhang LZ, Cui MG (2004) The effect of IBA on the Ca^{2+} absorption and Ca^{2+}-ATPase activity and their ultracytochemical localization in apple roots. *Acta Hortic* 636:211–219.
23. Noble D, Herchuelz A (2007) Role of Na/Ca exchange and the plasma membrane Ca^{2+}-ATPase in cell function. Conference on Na/Ca exchange. *EMBO Rep* 8:228–232.
24. Fujioka Y, Hiroe K, Matsuoka S (2000) Regulation kinetics of Na^+-Ca^{2+} exchange current in guinea-pig ventricular myocytes. *J Physiol* 529:611–623.
25. Dong H, Dunn J, Lytton J (2002) Stoichiometry of the Cardiac Na^+/Ca^{2+} exchanger NCX1.1 measured in transfected HEK cells. *Biophys J* 82:1943–1952.
26. Blackford S, Rea PA, Sanders D (1990) Voltage sensitivity of H^+/Ca^{2+} antiport in higher plant tonoplast suggests a role in vacuolar calcium accumulation. *J Biol Chem* 265: 9617–9620.
27. Brey RN, Rosen BP, Sorensen EN (1980) Cation/proton antiport systems in *Escherichia coli*. Properties of the potassium/proton antiporter. *J Biol Chem* 255:39–44.
28. Ebbs SD, Kochian LV (1998) Phytoextraction of zinc by oat (*Avena sativa*), barley (*Hordeum vulgare*), and Indian mustard (*Brassica juncea*). *Environ Sci Technol* 32: 802–806.